

Effect of Inorganic Acids and Salt on the Conduction Behaviour of PANI Composites by DFT and Experimental Studies

A. Ananda Jebakumar

Department of Chemistry, Government Polytechnic College for Women, Madurai,
Tamilnadu, India-625011

To Cite this Article

A. Ananda Jebakumar |, "Effect of Inorganic Acids and Salt on the Conduction Behaviour of PANI Composites by DFT and Experimental Studies " *Journal of Science and Technology, Vol. 03, Issue 06,- November-December 2018, pp68-89*

Article Info

Received: 27-10-2018 Revised: 07-11-2018 Accepted: 17-11-2018 Published: 27-11-2018

Abstract

Electroactive composite materials are a new generation of smart materials based on intrinsically conducting polymers like PANI. Here the computational and experimental study of polyaniline (PANI) composites of inorganic acids and salt are reported. The conductance is governed by charge mobility in the field produced between counter ions. Size, oxidation state and electron deficiency governs the conductance.

Keywords: PANI, Conductance, DFT, Spectral.

1. Introduction

Role of science is to alter nature for wellbeing [1]. Nowadays a great demand is created for energy harvesting, transport and storage [2]. In this path conductance plays a major role and modern synthetic metal, the conducting polymers are a great alternative for metal for its economic value, easy to process and maintenance [3]. Chemistry is fascinating because a small change in the chemicals gave a lot of variation in their property [4]. Such a slight as well as useful modification in the structure can be easily done through compositing [5]. In this background polyaniline (PANI) is a potential conducting polymer of academic and industrial value for designing [6]. PANI

has many forms and protonated form of neutral emeraldine base derived from aniline is mentioned as PANI [7] and it has lot of appreciations [8]. Role of research is to modify a material into a new one of the desired value [9]. In this sense understanding, the characters of the compound are essential. For the understanding of compounds, quantum mechanical calculation along with experimental study plays a major role [10]. DFT is a type of computational method by which the character such as structure and electronic effects can be accomplished in a good manner [11]. Among the experimental studies, spectra and electrical conductance are useful. In this scenario the properties as well the behaviour of PANI can be studied by composting. A vast majority of classes of compounds are available for the study of composites but inorganic and their salts may be helpful. Thus four different concentrations of PANI composites with inorganic acids and salts (IAS) are synthesised and studied by DFT, spectra and conductance. The inorganic acids studied are boric acid (BA), potassium dihydrogen ortho phosphate (PDHOP), molybdic acid (MA), phosphotungstic acid (PTA) and inorganic salt is sodium hypophosphate (SHP).

2. Experimental

2.1 Synthesis of PANI

All the chemicals used were of AR grade obtained from Merk, India and used as such.

10 g of aniline and 30.6 g of ammoniumperdisulphate were dissolved in 1M 250ml HCl separately and cooled them at 18°C. Ammoniumperdisulphate solution was added dropwise to the aniline solution with constant stirring for about 50 minutes. The content was kept aside for 12 hours and washed with water containing small amount of acetone. Then the content was filtered, dried at 80°C for 8 hours and stored in a polyethylene container. Water was used as solvent. The yield is 58%. Basic unit weight is 92. The percentage doping of HCl in PANI was measured by titrating a known amount of PANI with standard alkali [12].

2.2 Synthesis of Composites

Slurry was prepared by 400 mg of PANI and 100 mg of BA in 4 ml of DMSO for using mortar and pestle. The content was dried at 70 °C for 24 hrs. Weight loss method was employed to check the complete removal of DMSO from the mixture. The

composite was powdered and stored in a polyethylene container. The same procedure was repeated with 200, 300 and 400 mg of SA and others.

2.3 Computation

DFT studies were performed by B3LYP/ 6-31G** basis set in gas phase at 25 °C using firefly software [13] in i7 computer. TDDFT calculations were done using ORCA programme [14] by B3LYP/PBE0. Due to higher computational cost, the modeling studies were carried for each one unit of phenyl and phenylene rings for PANI and its composites.

2.4 Equipment

DC conductance was studied in Four Probe SES-Model DFP-RM. IR spectra were recorded in JASCO FT/IR-4600, UV-VIS in JASCO V-650 (DMSO Solvent) and Luminescence in Perkin Elmer, LS 45, excitation at 380 nm (DMSO Solvent). The spectral studies used 80% PANI.

2.5 Analysis

Regression analysis was carried out for conductance studies. The equations used were; for ideal- $y = y_0 + ax$; for real- $y = y_0 + ax + bx^2$. The ideal behaviour means expected. Pearson's correlation coefficients for ideal and real behaviours were calculated using software SPSS 16 [15].

3. Results and discussion

3.1 Stability and Structure

Due to higher computational cost the computations were studied for PANI-BA, PANI-PDHOP and PANI-SHP. The details about the stability and structure are given in Fig.1. Based on the stability values the phosphorus derivatives are more stable than boron. Among the phosphorous derivatives, PANI-PDHOP is more stable than PANI-SHP. The acid-salts are more stable than acids. The higher stability of PANI-PDHOP may be due to the bigger size of potassium over sodium atom and higher oxidation state of phosphorus in the later [16].

The structural parameters are given in Table 1. The order of binding of $H_{1'}$ with N_1 is PANI-PDHOP > PANI > PANI-BA > PANI-SHP with a magnitude of 28.8 % higher and 3.2 and 6.4% lower than that of PANI. There is no much difference in the bond length of other bonds and bond angles. The approaching angle of $H_{1'}-Cl_{2'}$ to the

polymer concerned is 24.4 and 16.3% acute and 18.6% obtuse than PANI. Based on the $\text{Cl}_2\text{-H}_1\text{-N}_1$ angle the position of H_1 changed from PANI by 1.3, 24.8 and 4.2% respectively for PANI-BA, PANI-PDHOP and PANI-SHP. Among them, both PANI-BA and PANI-SHP have a lower value than PANI. Based on the stability and structure the order of conductance is PANI-PDHOP > PANI-SHP > PANI-BA. The experimental conductance is almost reverse of the above order. So the thermodynamic stability has an adverse effect on the conductance due to larger separation between the energy bands [17].

3.2 Charge Density

Table 2 has the charge density values. The charge density of H_1 in PANI-PDHOP is increased from PANI by 38.5%, while for others the values are decreased. The same trend is repeated in the Cl_2 . This implies that H_1 strongly bind with the PANI skeleton in PANI-PDHOP. There is a small change in the charge density of other atoms. Further a significant change in the charge density of N_{14} , as it has a higher value than PANI. These results infer that there is a charge localisation at N_{14} . The charge density based order of conductance is PANI-PDHOP > PANI-BA > PANI-SHP. The order is changed from the experimental conductance and this may be due to electron localisation effect. Charge density reveals that phosphate is a better counter ion over borate. The difference from the experimental conductance can be accounted by the bulkiness of phosphate group and electron deficient nature of boron, which may cause higher conductance in the latter [18].

3.3 Dipole moment

The values of the dipole moment are given in Table 3. All the composites have a higher total dipole moment than PANI. This may be due to their acidic and salty nature. The rate of increase in the total dipole moment from PANI is 72.7, 29.8 and 21.1% respectively for PANI-SHP, PANI-PDHOP and PANI-BA. Along all the axis PANI-SHP has the highest value of dipole moment. For PANI-PDHOP the higher dipole moment value is in the x -axis. In PANI-BA the largest value of dipole moment is along the y -axis. Molecular polarizability does not match with the experimental conductance due to the higher electron localisation effect.

3.4 Molecular Orbital

Fig. 2 has the MO diagram of this system. The PANI-IAS formation can be observable from the MO diagrams as the MOs of the PANI-IAS are different from the PANI and their IAS. This implies that the compositing altered the energy levels in the PANI-IAS [19]. The MOs of the PANI-IAS are comparable with PANI than additives. There is a reasonable difference in the MOs of PANI-BA from others. For all the composites the LUMO is the π^* orbital of PANI. HOMO is concerned (Fig.3), for PANI-BA it is on N₁, PANI-PDHOP is Cl₂' and PANI-SHP is O₄". Unstable LUMO caused by the change in the orientation of a molecule may lead to higher conductance in PANI-BA [20].

3.5 TDDFT

Table 4 has the values of TDDFT. Both PANI-BA and PANI-SHP have one transition each in the visible region. PANI-BA has three transitions in the UV region. PANI-PDHOP has one transition in the UV region, while PANI-SHP has two transitions in the UV region. Based on the computed optical band gap the order of conductance is PANI-SHP > PANI-BA > PANI-PHOP. This order matches with the experimental. The two VIS region transitions of the PANI-IASs are within the PANI group. There is no charge transfer transition in the PANI-SHP. For others, the transition in the UV region is of charge transfer transition from IASs to PANI. The transitions of PANI-BA at 429.4, 310.5, 293.1 and 256 nm respectively for $n \rightarrow \pi^*$ of the polymer chain, $n \rightarrow \pi^*$ of Cl₂' to PANI, $n \rightarrow \pi^*$ of Cl₂' and O₆", O₄" to PANI and $n \rightarrow \pi^*$ of O₆", O₄" to PANI. For PANI-PDHOP, the only transition is $n \rightarrow \pi^*$ of O₂", O₄" to EB. The transitions of PANI-SHP at 443.7 nm, 322 nm and 299.4 nm are assigned for $n \rightarrow \pi^*$ of PANI, $\pi \rightarrow \pi^*$ of ES and combination of $n \rightarrow \pi^*$ and $\pi \rightarrow \pi^*$ of PANI.

3.6 Frontier Molecular Orbital

Values of the above parameters are given in Table 5. Based on the bandgap the order of conductance is PANI-PDHOP > PANI-SHP > PANI-BA > PANI. The chemical stability and Q^{Max} also follow the same order. This implies that the PANI-IAS has higher electron transfer ability over PANI and the above may be the order for the conductance. The higher value of PANI-PDHOP may be due to its higher oxidation state of phosphate. The values of PANI and PANI-BA are comparable. The additives have the order PDHOP > SHP > BA. BA can transfer one electron while other two

electron. $\Delta Q^{\text{Max}} = Q_{\text{composite}}^{\text{Max}} - (Q_{\text{PANI}}^{\text{Max}} + Q_{\text{additives}}^{\text{Max}})$ The ΔQ^{Max} values of PANI-BA and PANI-SHP have negative value, but PANI-PDHOP has two units higher. This implies that the PDHOP makes an impact on the PANI structure and enhance the PANI-PDHOP's electron sharing effect. All the derived parameters favoured the higher conductance for PANI-PDHOP.

3.7 Polarizability

The polarizability values are given in Table 6. PANI-PDHOP has very high γ and α -also higher along the z -axis. The order of polarizability is $\gamma > \alpha > \beta$. The polarizability order of conductance is similar to charge density. This implies that polarizability is not related to conductance.

3.8 Spectra

PANI-PTA has only spectral studies due to higher computational cost and difficulty in making pellets for electrical studies. The IR spectra show the presence of hydrogen bonding and C=N and C=C. Similarly, the electronic spectra indicate the presence of $n \rightarrow \pi^*$, $\pi \rightarrow \pi^*$ transition and polaron bands. The spectra are compared with computation with correction for gas phase. The fluorescence spectrum of PANI-IAS has two emissions in the visible region. The low energy emission is comparable for all the PANI-IAS. There is a significant difference in the higher energy emission except for PANI-MA and PANI-PTA.

3.9 Conductance

Conductance depends on thermodynamic stability, geometry, atomic charge density/atomic polarizability/electron localisation and molecular polarizability/dipole moment. The data related to the title are given in Table 7. The rate of change of conductance of the composites is a function of a , b and x . For PANI-BA the conductance decreased on the first addition of the BA and increased gradually for further additions. This may be due to the small size of the BA and the presence of electron deficient boron, which may reduce the electron density in the PANI and consequently increase the conductance. From the observation of the PANI-BA graph, the maximum deviation from the ideal behaviour is at 0.62 mole fraction of PANI. Both the slope of the ideal behaviour and the restoring effect calculated from the

parameter 'b' of the PANI-IAS have comparable values. The restoring force to maintain the ideal behaviour is 57% higher than that of 'a'.

For PANI-IAS such as PANI-PDHOP, PANI-SHP and PANI-MA the conductance decrease for each addition of IASs. The higher amount of decrease is observed in the case of PANI-SHP. It was expected that the conductance of the PANI-IAS is to be increased from the PANI, but in reality the conductance of the PANI-IAS are less than that of PANI. This may be due to the difference in the chemical behaviour of PANI and PANI in PANI-IAS. The difference in the chemical behaviour of PANI can be classified into two parts as, steric and electronic effects. The steric effect alters the geometry of the molecule and retards the flow of electron. Further, the electronic effect alters the conductance by localising the electrons. PANI-SHP conducts ten times lesser than other PANI-IAS. Both PANI-MA and PANI-PDHOP have comparable conductance. The order of conductance is PANI > PANI-BA > PANI-MA > PANI-PDHOP > PANI-SHP. The order of 'a', 'b' and 'x' are PANI-SHP > PANI-MA > PANI-PDHOP > PANI-BA and this is the order of deviation from the ideal or expected behaviour. At higher concentrations of PTA, PANI-PTA could not be made into a pellet.

4. Conclusion

In this work, computational and solid state behaviour of composites of PANI-inorganic salt and acids are reported. The conductance of the polymer followed hopping mechanism through the mobility of proton in the field produced between the polymer chain and counterion. The criteria for higher stability in the PANI-IAS are a bigger size, higher oxidation state, polarizability and salt form. Borate is a better counter ion than phosphate due to its small size and electron deficient nature. Unstable LUMO and higher oxidation state are related to the conductance.

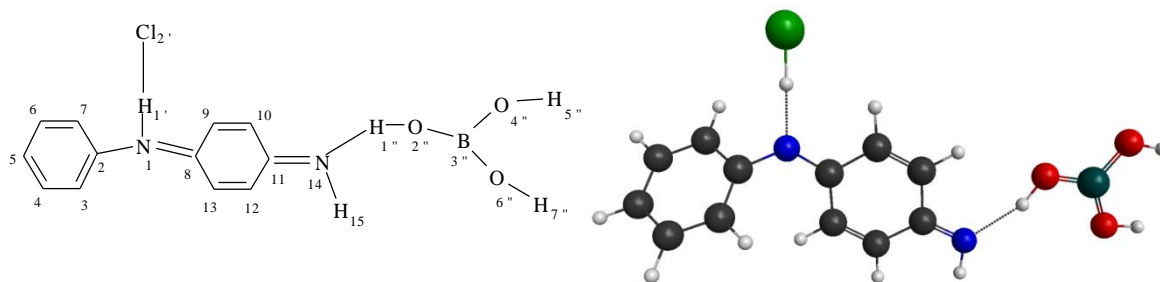
References

1. Jo Barton and Jules Pretty Environ. Sci. Technol. 2010, 44, 10, 3947–3955
2. Talita Greyling & Fiona Tregenna, Social Indicators Research, 2017, 131, 887–930.

3. Priscila Milani·Débora França, Aline Gambaro Balieiro·Roselena Faez, *Polímeros* 2017, 27, 3
4. Aimee M. Bryan, Luciano M. Santino, Yang Lu, Shinjita Acharya, and Julio M. D'Arcy, *Chem. Mater.* 2016, 28, 17, 5989–5998
5. Krishna C.Persaud, (2005) *Polymers for chemical sensing material today*, 8, 4, April, 38-44
6. Dimitra Sazou & Pravin P. Deshpande, *Chemical Papers*, 2017, 71, 459–487
7. Shiow-Jing Tang, An-Tsai Wang, Su-Yin Lin, Kuan-Yeh Huang, Chun-Chuen Yang, Jui-Ming Yeh & Kuan-Cheng Chiu *Polymer Journal*, 2011, 43, 667–675.
8. Boddula and Palaniappan Srinivasan *Journal of Catalysts* 2014 2314-5102.
9. M.F.Maitz *Biosurface and Biotribology*, 2015, 1, 3, 161-176
10. Imene Bekri-Abbes & Ezzeddine Srasra, (2011) Investigation of structure and conductivity properties of polyaniline synthesized by solid–solid reaction *Journal of Polymer Research* 18, 659–665
11. Giuseppe Felice Mangiatordi, Eric Brémond, and Carlo Adamo, *J. Chem. Theory Comput.* 2012, 8, 9, 3082–3088
12. Vogel, AI 1978, *A textbook of quantitative inorganic analysis*, Longman Inc., New York.
13. Granovsky, AA Firefly version 8, Schmidt, MW Baldrige, KK Boatz, JA Elbert, ST Gordon, MS Jensen, JH Koseki, S Matsunaga, N Nguyen, KA Su, S Windus, TL Dupuis, M & Montgomery, JA *Journal of computational chemistry*, 1993, 14, 11, 1347-1363.

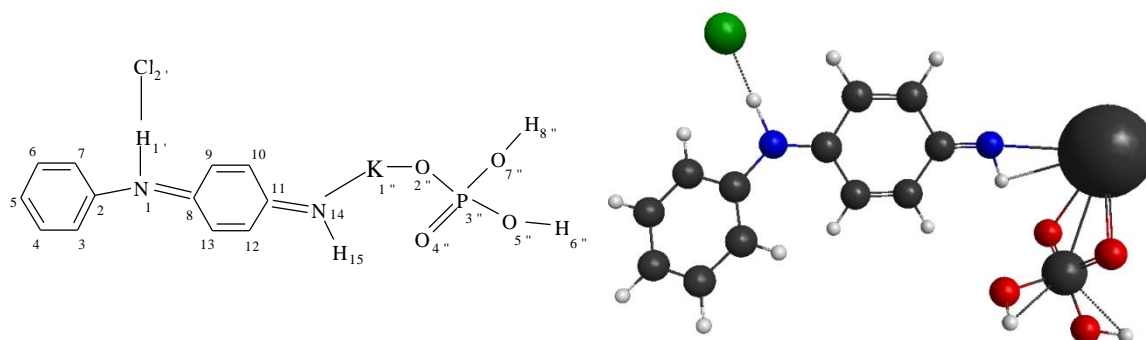
14. Neese, F Computational Molecular Science, 2012, 2, 1, 73-78
15. Sabine Landau and Brian S. Everitt, 2014, A Handbook of Statistical Analyses using SPSS, Chapman & Hall/CRC Press.
16. Duba, A & Nicholls, A 'Science Letters, 1973, 18, 1, 59-64.
17. Xie, Y Yu, HT Yi, TF Wang, Q Song, QS Lou, M & Zhu, YR, Journal of Materials Chemistry A, 2010, 3, 39, 19728-19737
18. He, H Pandey, R Boustani, I & Karna, SP The Journal of Physical Chemistry C, 2010, 114, 9, 4149-4152
19. Kitchin, CR 1995, Optical astronomical spectroscopy, Taylor & Francis, London
20. Xue, Y & Mansoori, GA Intrnational Journal of Nanoscience, 2008, 7, 1, 63-72.

Figure 1 : Structure and Thermodynamic Stability



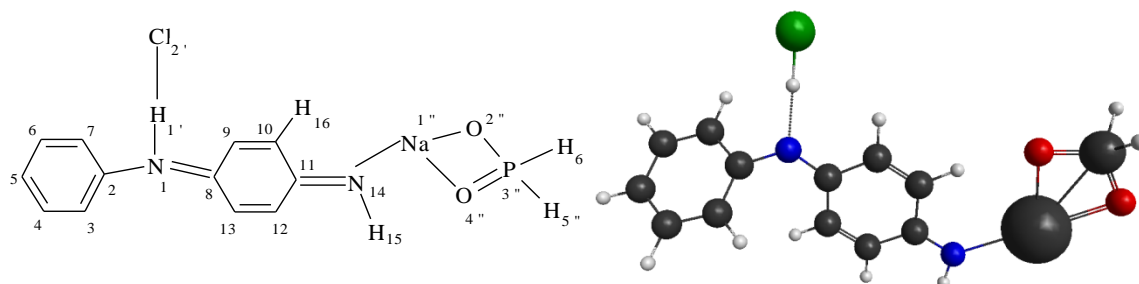
ES-BA

(ES-BA- (ES+BA) = -36.4156 kJ/mole)



ES-PDHOP

(ES-PDHOP- (ES+PDHOP) = -93.599 kJ/mole)



ES-SHP

(ES-SHP- (ES+ SHP) = -84.1472 kJ/mole)

C-Black; H-White; O- Red; N-Blue; Cl-Green; K,P,Na

Figure 2: MO Diagram

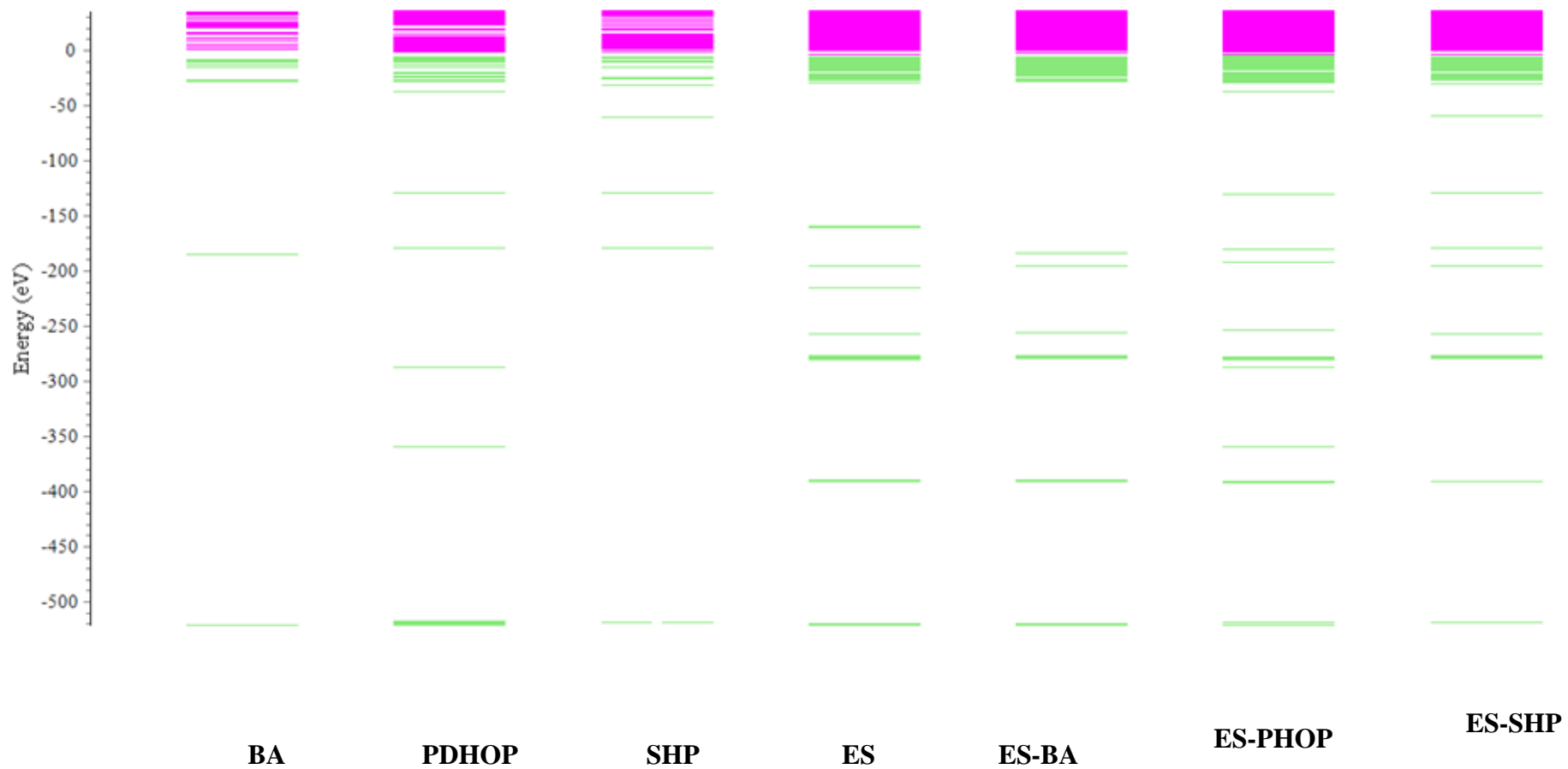
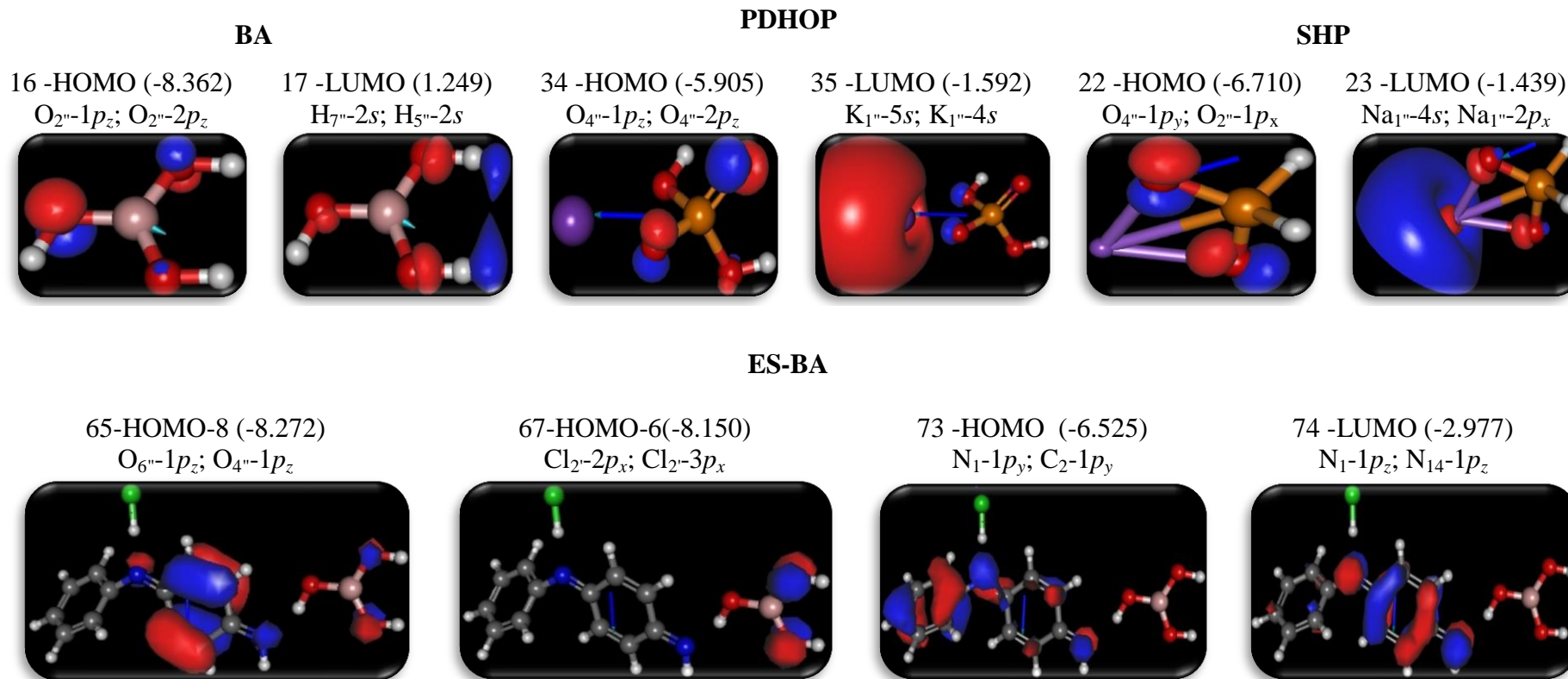
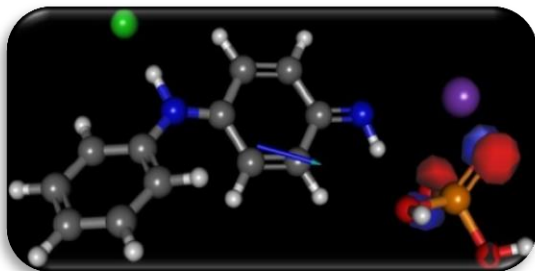


Figure 3: MO Number, Name, Energy(eV) and AO Contribution to MO

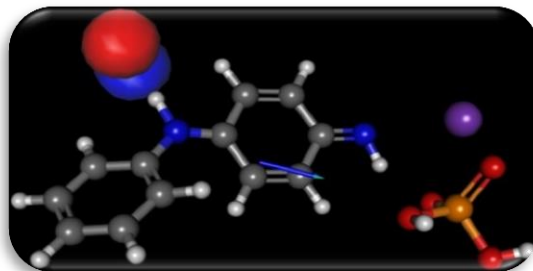


ES-PDHOP

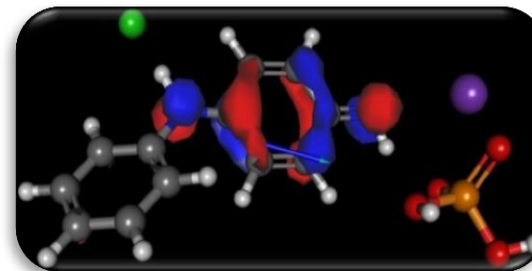
88-HOMO-3 (-6.732)
 $O_{2''}-1p_z$; $O_{4''}-1p_y$



91-HOMO (-5.192)
 Cl_2-2p_z ; Cl_2-3p_z

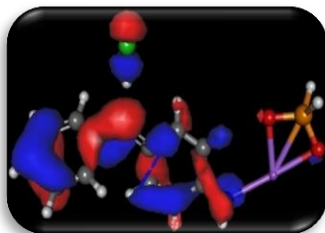


92-LUMO (-3.701)
 $N_{14}-1p_z$; N_1-1p_z

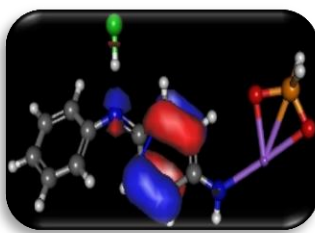


ES-SHP

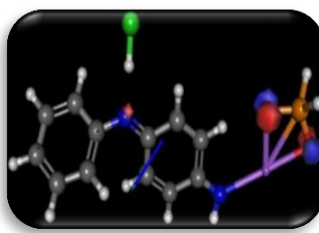
69 -HOMO-10 (-8.661)
 N_1-1p_y



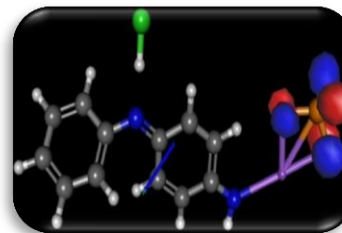
70 -HOMO-9 (-8.493)
 $C_{13}-1p_z$; $C_{12}-1p_z$



77 -HOMO-2 (-6.767)
 N_1-1p_y ; C_5-1p_z



79 -HOMO (-6.490)
 $O_{4''}-1p_z$; $O_{4''}-2p_z$



80 -LUMO (-3.412)
 N_1-1p_z ; $N_{14}-1p_z$

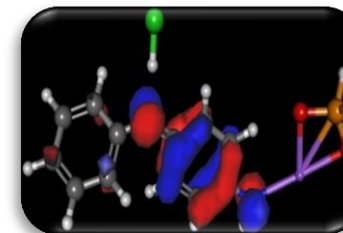


Table 1: Structural Parameters

| Atom Pair | Bond Length (Å) | | | Atom Pair | Bond Angle (°) | | | Atom Pair | Dihedral Angle (°) | | |
|---------------------------------|-----------------|----------|--------|---|----------------|----------|--------|---|--------------------|----------|---------|
| | ES-BA | ES-PDHOP | ES-SPH | | ES-BA | ES-PDHOP | ES-SHP | | ES-BA | ES-PDHOP | ES-SHP |
| H ₁ -Cl ₂ | 1.3591 | 1.7166 | 1.3461 | Cl ₂ -H ₁ -N ₁ | 177.73 | 175.34 | 177.22 | Cl ₂ -H ₁ -N ₁ -C ₂ | -69.26 | -98.13 | -62.57 |
| N ₁ -H ₁ | 1.6720 | 1.1533 | 1.7244 | H ₁ -N ₁ -C ₂ | 114.20 | 114.37 | 113.80 | H ₁ -N ₁ -C ₂ -C ₇ | 40.05 | 30.51 | 38.84 |
| N ₁ -C ₂ | 1.4046 | 1.4096 | 1.4022 | H ₁ -N ₁ -C ₈ | 120.91 | 116.44 | 121.25 | H ₁ -N ₁ -C ₈ -C ₉ | 9.52 | 11.40 | 9.73 |
| N ₁ -C ₈ | 1.3032 | 1.3136 | 1.3033 | N ₁ -C ₂ -C ₇ | 117.58 | 116.68 | 117.47 | N ₁ -C ₂ -C ₇ -C ₆ | -177.83 | -178.29 | -178.04 |
| C ₂ -C ₃ | 1.4077 | 1.4051 | 1.4087 | C ₂ -C ₃ -C ₄ | 120.01 | 119.49 | 120.00 | C ₂ -N ₁ -C ₈ -C ₁₃ | 9.08 | 7.559 | 9.70 |
| C ₂ -C ₇ | 1.4066 | 1.4054 | 1.4075 | C ₃ -C ₄ -C ₅ | 120.39 | 120.37 | 120.37 | C ₂ -C ₃ -C ₄ -C ₅ | 0.20 | -0.429 | 0.35 |
| C ₃ -C ₄ | 1.3933 | 1.3922 | 1.3929 | C ₅ -C ₆ -C ₇ | 120.41 | 120.44 | 120.40 | C ₃ -C ₂ -C ₇ -C ₆ | -3.05 | -2.947 | -3.29 |
| C ₄ -C ₅ | 1.3959 | 1.3970 | 1.3961 | C ₆ -C ₇ -C ₂ | 120.06 | 119.45 | 120.05 | C ₄ -C ₃ -C ₂ -C ₇ | 1.94 | 2.515 | 1.98 |
| C ₅ -C ₆ | 1.3977 | 1.3971 | 1.3980 | C ₇ -C ₂ -C ₃ | 119.32 | 120.24 | 119.31 | C ₅ -C ₆ -C ₇ -C ₂ | 2.038 | 1.298 | 2.28 |
| C ₆ -C ₇ | 1.3911 | 1.3914 | 1.3906 | C ₈ -N ₁ -C ₂ | 124.82 | 128.99 | 124.90 | C ₇ -C ₂ -N ₁ -C ₈ | -137.40 | -144.31 | -139.06 |

| | | | | | | | | | | | |
|----------------------------------|--------|--------|--------|---|--------|---------|--------|--|--------|----------|---------|
| C ₈ -C ₁₃ | 1.4682 | 1.4566 | 1.4679 | C ₉ -C ₁₀ -C ₁₁ | 121.11 | 121.70 | 120.52 | C ₈ -C ₁₃ -C ₁₂ -C ₁₁ | 0.00 | 0.00 | 0.00 |
| C ₉ -C ₁₀ | 1.3476 | 1.3480 | 1.3493 | C ₁₀ -C ₁₁ -C ₁₂ | 117.05 | 116.97 | 117.31 | C ₉ -C ₁₀ -C ₁₁ -C ₁₂ | 1.39 | 0.00 | 1.09 |
| C ₁₀ -C ₁₁ | 1.4674 | 1.4651 | 1.4660 | C ₁₁ -C ₁₂ -C ₁₃ | 121.79 | 121.60 | 121.91 | C ₁₀ -C ₁₁ -C ₁₂ -C ₁₃ | -2.59 | -2.047 | -2.48 |
| C ₁₁ -C ₁₂ | 1.4691 | 1.4724 | 1.4688 | C ₁₂ -C ₁₃ -C ₈ | 120.87 | 120.34 | 120.72 | C ₁₂ -C ₁₁ -N ₁₄ - H ₁₅ | -0.85 | 0.00 | -0.99 |
| C ₁₁ -N ₁₄ | 1.2925 | 1.2906 | 1.3001 | C ₁₃ -C ₈ -N ₁ | 124.94 | 124.363 | 125.08 | C ₁₂ -C ₁₃ -C ₈ -N ₁ | -180 | -178.441 | -180.00 |
| C ₁₂ -C ₁₃ | 1.3472 | 1.3494 | 1.3472 | N ₁₄ -C ₁₁ -C ₁₂ | 124.08 | 122.797 | 122.66 | C ₁₃ -C ₁₂ -C ₁₁ -N ₁₄ | 178.66 | 180 | 178.95 |
| N ₁₄ -H ₁₅ | 1.0230 | 1.0386 | 1.0228 | H ₁₅ -N ₁₄ -C ₁₁ | 111.97 | 110.665 | 110.54 | | | | |

Table 2 :Mulliken's Atomic Charge Density

| ES-BA | | ES-PDHOP | | ES-SPH | |
|------------------|---------------|------------------|---------------|------------------|---------------|
| Atom | Charge | Atom | Charge | Atom | Charge |
| H _{1'} | 0.1804 | H _{1'} | 0.2589 | H _{1'} | 0.1740 |
| Cl _{2'} | -0.3049 | Cl _{2'} | -0.6073 | Cl _{2'} | -0.2849 |
| N ₁ | -0.6056 | N ₁ | -0.6007 | N ₁ | -0.5955 |
| C ₂ | 0.2475 | C ₂ | 0.2567 | C ₂ | 0.2482 |
| C ₃ | -0.0978 | C ₃ | -0.0945 | C ₃ | -0.0979 |
| C ₄ | -0.0960 | C ₄ | -0.0986 | C ₄ | -0.0960 |
| C ₅ | -0.0772 | C ₅ | -0.0718 | C ₅ | -0.0760 |
| C ₆ | -0.0924 | C ₆ | -0.0939 | C ₆ | -0.0919 |
| C ₇ | -0.0915 | C ₇ | -0.0896 | C ₇ | -0.0909 |
| C ₈ | 0.3346 | C ₈ | 0.3519 | C ₈ | 0.3301 |
| C ₉ | -0.1055 | C ₉ | -0.1059 | C ₉ | -0.1167 |
| C ₁₀ | -0.0895 | C ₁₀ | -0.0696 | C ₁₀ | -0.0924 |
| C ₁₁ | 0.3172 | C ₁₁ | 0.3009 | C ₁₁ | 0.3281 |
| C ₁₂ | -0.1060 | C ₁₂ | -0.0897 | C ₁₂ | -0.1079 |
| C ₁₃ | -0.0927 | C ₁₃ | -0.1017 | C ₁₃ | -0.0898 |
| N ₁₄ | -0.5900 | N ₁₄ | -0.6363 | N ₁₄ | -0.6310 |
| H ₁₅ | 0.2421 | H ₁₅ | 0.3162 | H ₁₅ | 0.2474 |

Table 3: Dipole moment (D)

| | μ_x | μ_y | μ_z | μ_{Total} |
|----------|---------|---------|---------|----------------------|
| BA | 0.9396 | -2.9534 | 0.0000 | 3.0993 |
| ES-BA | -0.1208 | 7.8225 | -0.7469 | 7.8590 |
| PDHOP | -9.0437 | 1.9199 | -3.3802 | 9.8437 |
| ES-PDHOP | 8.1321 | 2.0091 | -0.8563 | 8.4202 |
| SHP | -4.1386 | 2.8157 | -0.0522 | 5.0059 |
| ES-SHP | -5.4426 | 9.4804 | 2.4655 | 11.2062 |

Table 4: TDDFT**ES-BA**

| Wave Length (nm) | Oscillatory Strength | Orbital | % Contribution |
|-----------------------------|---------------------------------|----------------|-----------------------|
| 429.4 | 0.2462 | 73a → 74a | 76.82 |
| 310.5 | 0.1368 | 67a → 74a | 35.38 |
| 293.1 | 0.3283 | 65a → 74a | 37.58 |
| | | 67a → 74a | 26.77 |
| 256 | 0.6363 | 65a → 74a | 34.12 |

ES-PDHOP

| Wave Length (nm) | Oscillatory Strength | Orbital | % Contribution |
|-----------------------------|---------------------------------|----------------|-----------------------|
| 362.8 | 0.6504 | 88a → 92a | 69.62 |

ES-SHP

| Wave Length (nm) | Oscillatory Strength | Orbital | % Contribution |
|-----------------------------|---------------------------------|----------------|-----------------------|
| 443.7 | 0.2555 | 77a → 80a | 77.04 |
| 322 | 0.1362 | 70a → 80a | 40.28 |
| 299.4 | 0.3009 | 69a → 80a | 42.04 |
| | | 70a → 80a | 40.64 |

Table 5: Frontier Molecular Orbital

| | eV | | | | | | | | Q ^{Max} |
|----------|----------|----------------------|-------------------|-------------------------------|-------------------|-----------------|---------------------|-----|------------------|
| | Band Gap | Ionisation potential | Electron affinity | Electronic chemical potential | Chemical hardness | Global softness | Electrophilic index | EN | |
| BA | 9.6 | 8.4 | -1.2 | -3.6 | 4.8 | 0.2 | 30.4 | 3.6 | 0.7 |
| PDHOP | 4.3 | 5.9 | 1.6 | -3.7 | 2.2 | 0.5 | 15.2 | 3.7 | 1.7 |
| SHP | 5.3 | 6.7 | 1.4 | -4.1 | 2.6 | 0.4 | 21.9 | 4.1 | 1.5 |
| ES- BA | 3.5 | 6.5 | 3.0 | -4.8 | 1.8 | 0.6 | 20.0 | 4.8 | 2.7 |
| ES-PDHOP | 1.5 | 5.2 | 3.7 | -4.4 | 0.7 | 1.3 | 7.4 | 4.4 | 6.0 |
| ES- SHP | 3.1 | 6.5 | 3.4 | -5.0 | 1.5 | 0.6 | 18.9 | 5.0 | 3.2 |

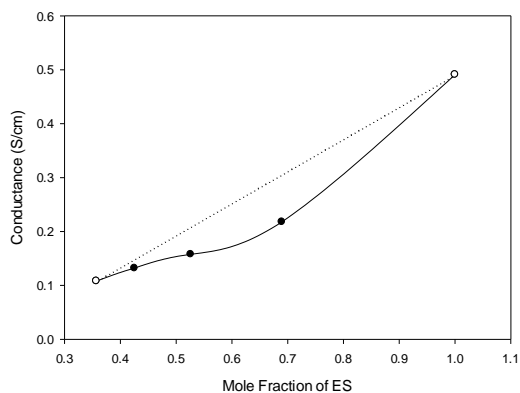
Table 6: Polarisability (Au)

| Axis | BA | ES-BA | PDHOP | ES-PDHOP | SHP | ES-SHP |
|-----------------|-------------------------|--------------|--------------|-----------------|------------|---------------|
| μ_z | -1.18×10^{-15} | -0.294 | -1.33 | -0.337 | -0.0206 | 0.970 |
| α_{xz} | -3.2610^{-12} | -1.51 | 0.713 | 22.5 | 0.148 | 13.5 |
| α_{yz} | 7.55×10^{-12} | 12.0 | -0.291 | -23.5 | 0.0119 | 3.70 |
| α_{zz} | 12.7 | 86.7 | 34.0 | 105 | 29.1 | 102 |
| β_{xzz} | -0.494 | -15.0 | 112 | -218 | 91.1 | -96.0 |
| β_{yzz} | 0397 | -16.1 | -21.2 | 95.0 | -62.6 | -84.9 |
| β_{zzz} | 1.23×10^{-09} | -6.48 | 37.2 | -11.5 | 3.44 | -68.9 |
| γ_{zzzz} | 248 | 966 | 7750 | 8800 | 5660 | 7700 |

Table 7: Conductance

ES-BA

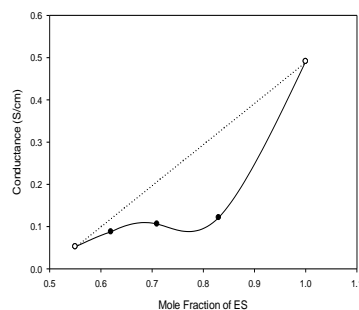
| Mole Fraction of ES | Conductance S/cm |
|---------------------|------------------|
| 1.0000 | 0.4910 |
| 0.7771 | 0.1797 |
| 0.6354 | 0.2491 |
| 0.5375 | 0.3020 |
| 0.4657 | 0.3579 |



| | R | y₀ | a | b |
|--------------|----------|----------------------|----------|----------|
| Ideal | 1.0 | -0.1047 | 0.5957 | - |
| Real | 0.9987 | 0.1946 | -0.5059 | 0.8006 |

ES-PDHOP

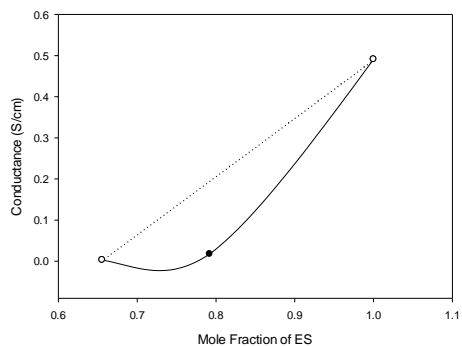
| Mole Fraction of ES | Conductance S/cm |
|---------------------|------------------|
| 1.0000 | 0.4910 |
| 0.8301 | 0.1211 |
| 0.7096 | 0.1060 |
| 0.6196 | 0.0875 |
| 0.5499 | 0.0522 |



| | R | y₀ | a | b |
|--------------|----------|----------------------|----------|----------|
| Ideal | 1.0 | -0.4838 | 0.9748 | - |
| Real | 0.9770 | 1.3866 | -4.1602 | 3.2499 |

ES-SHP

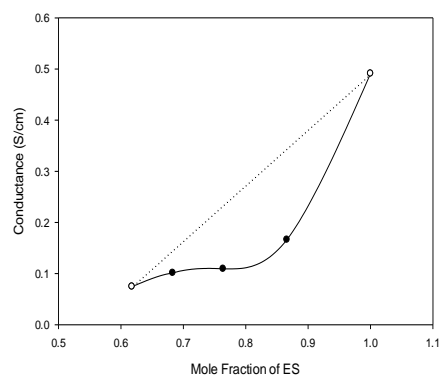
| Mole Fraction of ES | Conductance S/cm |
|---------------------|------------------|
| 1.0000 | 0.4910 |
| 0.7919 | 0.0175 |
| 0.6555 | 0.002907 |



| | R | y ₀ | a | b |
|--------------|-----|----------------|---------|--------|
| Ideal | 1.0 | -0.9259 | 1.4169 | - |
| Real | 1.0 | 3.2007 | -9.0049 | 6.2952 |

ES-MA

| Mole Fraction of ES | Conductance S/cm |
|---------------------|------------------|
| 1.0000 | 0.4910 |
| 0.8660 | 0.1660 |
| 0.7636 | 0.1092 |
| 0.6829 | 0.1011 |
| 0.6176 | 0.0745 |



| | R | y ₀ | a | b |
|--------------|--------|----------------|---------|--------|
| Ideal | 1.0 | -0.5983 | 1.0893 | - |
| Real | 0.9876 | 2.1565 | -6.0143 | 4.3373 |